Joint Conference of 1996 International Computer Symposium
December 19~21, Kaohsiung, Taiwan, R.O.C.

Detection and Concealment of Transmission Errors in MPEG Images[+]

Han-Chiang Shyu[#] and Jin-Jang Leou[#@]

#Institute of Computer Science and Information Engineering
National Chung Cheng University
Chiayi, Taiwan 621, Republic of China

ABSTRACT

In this study, the detection and concealment approach to transmission errors in MPEG-2 images is proposed. For entropy-coded MPEG images, a transmission error in a codeword may cause the current codeword and its subsequent codewords within a slice to be misinterpreted, resulting in a great degradation of the received images. In the proposed approach, transmission errors within a slice of an MPEG image are detected by two successive procedures. When a block is determined to be a corrupted/lost one, the proposed GA approach to error concealment is employed to conceal the corrupted/lost block. Based on the simulation results obtained in this study, the proposed approach can recover high-quality MPEG images from the corresponding corrupted MPEG images. This shows the feasibility of the proposed approach.

1. INTRODUCTION

To reduce transmission bit rate or storage capacity, many compression techniques have been developed for wide scope of applications, such as videoconferencing, videophones, facsimile transmission, high definition TV, and interactive TV [1], [2]. Standardization of image compression techniques has become an important issue of interoperability of equipment from different manufacturers. The high-performance compression standard for moving pictures and associated audio is the MPEG (Motion Picture Experts Group) Compression Standard [3], [4]. MPEG is an ISO standard and its premise is that a video signal (typically 720x480 in size) and its associated audio can be compressed to a bit rate between 5 and 10 Mbit/s. The MPEG coded format utilizes the discrete cosine transform (DCT) for reduction of spatial redundancy, forward/backward motion compensation for reduction of temporal redundancy, and variable-length code (VLC) for reduction of transmitted data.

Because MPEG images are entropy-coded, a transmission error in a codeword may cause the current codeword and its subsequent codewords to be misinterpreted, resulting in a great degradation of the received images. To limit the propagation effect of transmission errors, each of the top four layers of the MPEG hierarchical structure, namely, Video Sequence, Group of Pictures, Picture, and Slice, is ahead with a 32-bit start code (a synchronization codeword). After the decoder receives any start code, the decoder will be resynchronized. Even with start codes, a transmission error will affect the current codeword and its subsequent codewords within each corrupted slice and will greatly degrade the quality of the received MPEG images.

In general, three main approaches to eliminating the image quality degradation effect due to transmission errors include: (1) the channel coding approach [5], (2) the detection and correction approach [6]-[8], and (3) the detection and concealment approach [9]-[14]. For the channel coding approach, some error correction codes are used to encode images such that transmission errors can be detected and corrected by using additional side information [5]. Although it can detect and/or correct transmission errors to a small extent, it will moderately increase the transmission bit rate. For the detection and correction approach, based on the redundancy information inherent in neighboring pixels, the constraints imposed on compressed image data, and the accompanied statistical property changes of received pixels owing to transmission errors, transmission errors can be directly detected and corrected [6]-[8]. Because the total number of bits between two successive start codes within MPEG images is too large, the detection and correction approach is computationally expensive for transmission errors in MPEG images.

In ISO/IEC Recommendation H.262 (ISO/IEC 13818-2) [4], several error resilience techniques, namely, error concealment, spatial localization, and temporal localization, have been addressed. Error concealment techniques will hide the visual effect of losses/errors once they occur. Based on the information used for concealment,

+ This work was supported partially by National Science Council, Republic of China under Grant NSC 85-2213-E-194-004.

@ Author to whom all correspondence should be addressed. E-mail:jjleou@cs.ccu.edu.tw, Tel: 886-5-2720411 Ext. 6014, Fax: 886-5-2720859.

the error concealment methods [9]-[14] can be generally divided into three categories: (1) the spatial (frequency/spectral) error concealment methods, (2) the temporal error concealment methods, and (3) the hybrid error concealment methods. However, within most error concealment methods, it is assumed that transmission errors (error bits, corrupted/lost cells, corrupted/lost packets) are either detected or known. Additionally, they are lacking in a good objective performance measurement for error concealment. In this study, the detection and concealment approach to transmission errors in MPEG images is proposed. A good performance measure (objective function) for error concealment is also proposed. The objective is to detect and conceal transmission errors in MPEG images, without increasing the transmission bit rate.

Because "slice" is the smallest synchronization unit in MPEG images, by utilizing the vertical position (macroblock-based) included within the slice_start_code, each slice_start_code containing a single-bit error can be detected and corrected effectively. After a slice is located, transmission errors within the slice are detected by two successive procedures: (1) whether the slice is corrupted or not is determined by checking a set of error-checking conditions, and (2) the precise location of the first corrupted block within the corrupted slice is verified by a backtracking procedure. To conceal a corrupted/lost block can be formulated as an optimization problem. Here genetic algorithms (GAs) [15] are employed to conceal the corrupted blocks. Genetic algorithms (GAs) represent a class of highly parallel adaptive search processes for solving a wide range of search, optimization, and machine learning problems. Compared with conventional optimization methods, GAs can find near global optimal solutions over a limited number of strings (chromosomes).

In this study, a transmission error may be a single-bit error or a burst error. However, to simplify the processing steps in the proposed approach, a burst error containing several error bit segments is treated as several transmission errors, i.e., a transmission error may be either a single-bit error or a burst error containing N successive error bits. And it is also assumed that: (1) the sequence, group of pictures, and picture headers of MPEG images are correctly received; (2) within an MPEG image, each slice_start_code will contain at most a single-bit error; (3) the restricted slice structure, where all macroblocks in an MPEG image are enclosed by slices, is employed and each macroblock row in an MPEG image contains a single slice; and (4) only single MPEG video bitstream is transmitted.

In the remainder of this paper, the proposed detection and concealment approach to transmission errors in MPEG images is addressed in Section 2. Simulation results are included in Section 3, followed by concluding remarks.

2. DETECTION AND CONCEALMENT OF TRANSMISSION ERRORS IN MPEG IMAGES

2.1 Proposed Error Detection Approach

Based on the syntax of MPEG [4], the top two levels can be translated to be two decoding control procedures, namely, Decode_sequence and Decode_gop in the MPEG decoder, which are illustrated in Figs. 1 and 2, respectively. The proposed error detection and concealment approach, embedded in the Decode_picture procedure, is illustrated in Fig. 3.

For the 8-connected neighboring blocks of a corrupted/lost block, a block is called a correctly-received block if it is determined as a good block by the proposed error detection approach. Otherwise, it is called a corrupted block. A corrupted block becomes a concealed block if it has been concealed. Both the correctly-received and concealed neighboring blocks of a corrupted/lost block are called the believable neighboring blocks of the corrupted/lost block.

Here it is assumed that each slice_start_code will contain at most a single-bit error. As shown in Fig. 3, the slice_start_code determination procedure is used to find each slice_start_code. By performing the slice_start_code determination procedure, the start position of each slice within a picture can be correctly recognized even a single-bit error occurs on the slice_start_code. The details can be found in Shyu [16], and are thus omitted here.

After all the slice_start_codes within an MPEG image are detected, the transmission errors within a slice will be detected. Here transmission errors within a slice in an MPEG-2 image are detected by two successive procedures: (1) whether the slice is corrupted or not is determined by checking a set of error-checking conditions, and (2) the precise location of the first corrupted block within the corrupted slice is verified by a backtracking procedure. The set of error-checking conditions are derived from the constraints imposed on the MPEG-2 video bitstream syntax. The precise location of the first corrupted block within a corrupted slice is determined by using the redundant information inherent within MPEG images, the accompanied property changes of compressed image data and the reconstructed images owing to transmission errors, and several statistical measures.

The set of error-checking conditions is listed as follows:

(1) An invalid codeword for macroblock_address_increment, macroblock_type, coded_block_pattern, motion_code, or DCT coefficients is found.
(2) The total number of decoded DCT coefficients within a block is larger than 64.
(3) The macroblock_address_increment is not equal to 1 in an I-picture.
(4) The total number of decoded macroblocks within a slice is not exactly equal to the expected number of macroblocks within a slice.
(5) The total number of decoded blocks within a slice is not exactly equal to the expected number of blocks within a slice.

(6) Physically impossible image data are decoded. For example, a magnitude beyond the range of allowed values is detected.

It is noted that the first procedure might not determine the precise position of the first corrupted block within a slice. So the second procedure of the proposed error detection approach is used to determine the true first corrupted macroblock within a corrupted slice by backtracking from the first corrupted block detected by the first procedure. Finally, the true first corrupted block and its subsequent blocks within the corrupted slice are required to be concealed.

First, a measure, namely, the average intersample difference (AID) of a block C (N×M in size), is first employed in this study to check whether a block is corrupted or not. AID is given by:

$$AID(C) = \frac{\sum_{y=0}^{N-1}\sum_{x=1}^{M-1}|C(x,y)-C(x-1,y)| + \sum_{x=0}^{M-1}\sum_{y=1}^{N-1}|C(x,y)-C(x,y-1)|}{N\times(M-1)+M\times(N-1)}, \quad (1)$$

where C(x,y)is the pixel value of position (x,y) within the block C (using a local coordinate system). Second, a measure, namely, the average intersample difference of the block boundary (AIDB) between the block C and all the believable neighboring blocks is given by:

$$AIDB(C) = \frac{1}{|BN_C \cap N_C|}\sum_{B_i \in BN_C \cap N_C} ABD(C, B_i), \quad (2)$$

where $|X|$ denotes the total number of blocks within the set X, BN_c is the set containing all the believable neighboring blocks of the block C, N_c is the set containing all the 4-connected neighboring blocks of the block C, and

$$ABD(C,X) = \begin{cases} \frac{1}{8}\sum_{i=0}^{7}|C(0,i)-X(7,i)|, \\ \quad \textit{if X is the top neighboring block of C,} \\ \frac{1}{8}\sum_{i=0}^{7}|C(7,i)-X(0,i)|, \\ \quad \textit{if X is the bottom neighboring block of C,} \\ \frac{1}{8}\sum_{i=0}^{7}|C(i,0)-X(i,7)|, \\ \quad \textit{if X is the left neighboring block of C,} \\ \frac{1}{8}\sum_{i=0}^{7}|C(i,7)-X(i,0)|, \\ \quad \textit{if X is the right neighboring block of C.} \end{cases} \quad (3)$$

AIDB(C; BN_c) is also employed to check whether a block is corrupted or not. Third, several statistical measures for evaluating the characteristic differences between a block and its 4-connected believable neighboring blocks, namely, the average AID difference (AAIDD), the average mean difference (AMD), and the average variance difference (AVD) are given, respectively, by:

$$AAIDD(C) = \frac{1}{|BN_C|}\sum_{B_i \in BN_C}|AID(C) - AID(B_i)|, \quad (4)$$

$$AMD(C) = \frac{1}{|BN_C|}\sum_{B_i \in BN_C}|Mean(C) - Mean(B_i)|, \quad (5)$$

$$AVD(C) = \frac{1}{|BN_C|}\sum_{B_i \in BN_C}|Variance(C) - Variance(B_i)|. \quad (6)$$

Here for the above five measures, five corresponding thresholds, namely, Th_{AID}, Th_{AIDB}, Th_{AAIDD}, Th_{AMD}, and Th_{AVD} are set to (50, 65, 50, 70, 5000) for the Y component and identically (20, 30, 15, 30, 1300) for the C_b and C_r components. If any of the five measures of a block is larger than the corresponding threshold, the block will be determined as a corrupted block. And if any block of a macroblock is corrupted, the macroblock is determined as a corrupted one. It is noted that because the first procedure of the proposed error detection approach might not detect each corrupted slice, a double checking method is embedded in the second procedure to re-check each "good" slice determined by the first procedure.

2.2 Proposed Genetic Algorithm Approach to Error Concealment

After the locations of the corrupted/lost blocks are determined, for a corrupted/lost block, GAs (genetic algorithms) will be employed to conceal (estimate the contents of) each corrupted/lost block. In this study, the 64 integer pixel values of a block (Y, C_b or C_r) will be represented as a chromosome (binary bit string) in GAs. Each pixel is represented as a 8-bit binary bit string and the total number of bits of the chromosome is 512, i.e., the whole solution space of a corrupted/lost block (Y, C_b or C_r) contains 2^{512} possible solutions. In this study, the population size is set to 60 and the maximum number of iterations MAXPOP is set to 40. Additionally, several other issues must be considered as follows.

A. Initial population

The initial population may be randomly-selected or user-specified. In this study, the initial population contains both randomly-selected and user-specified chromosomes, where the user-specified chromosomes are specified by using the information from the spatial, spectral, and temporal domains.

B. Fitness (objective) function

The fitness (objective) function in GAs is used to evaluate the goodness of a concealed block, which is formed by linearly-weighted combining a temporal fitness function and a spatial fitness function. For the temporal fitness function, the shadow block difference (SBD) of a corrupted/lost block C is given by:

$$SBD(C, SB) = \frac{1}{64}\sum_{i=1}^{8}\sum_{j=1}^{8}\left|C_c(i,j) - SB(i,j)\right|, \quad (7)$$

where C_c is the concealed block and SB is the shadow block of C. A shadow block (SB) is constructed by linearly-weighted combining all the motion-compensated blocks using the FMVs and BMVs of the believable neighboring blocks of a corrupted/lost block C, i.e.,

$$SB(C) = \frac{\left|S_{FMV}(C)\right|}{\left|S_{FMV}(C) \cup S_{BMV}(C)\right|} B_f(C) + \frac{\left|S_{BMV}(C)\right|}{\left|S_{FMV}(C) \cup S_{BMV}(C)\right|} B_b(C), \quad (8)$$

where $S_{FMV}(C)$ and $S_{BMV}(C)$ are the sets of the forward motion vectors and backward motion vectors for the believable neighboring blocks of a corrupted/lost block C, respectively. $B_f(C)$ and $B_b(C)$ are the motion compensated blocks retrieved from the previous and proceeding I-pictures or P-pictures using the "mean" motion vectors of $S_{FMV}(C)$ and $S_{BMV}(C)$, respectively. The spatial fitness function is formed by linearly-weighted combining the five performance measures, namely, AID, AIDB, AAIDD, AMD, and AVD. As a summary, the proposed fitness function for GAs is given by:

$$f(\cdot) = w_{temporal} \times f_{temporal}(\cdot) + w_{spatial} \times f_{spatial}(\cdot), \quad (10)$$

$$f_{temporal}(\cdot) = SBD(C, SB), \quad (11)$$

$$f_{spatial}(\cdot) = w_1 \times \left[AID(C{:}*)\right]^2 + w_2 \times \left[AIDB(C)\right]^2 + w_3 \times \left[AAIDD(C)\right]^2 + w_4 \times AMD(C{:}*) + w_5 \times AVD(C{:}*), \quad (12)$$

where $w_{temporal}$ and $w_{spatial}$ are two weighting coefficients with $w_{temporal} + w_{spatial} = 1$, and w_1, w_2, w_3, w_4, and w_5 are five weighting coefficients with $w_1 + w_2 + w_3 + w_4 + w_5 = 1$. For an I-picture, ($w_{temporal}$, $w_{spatial}$) are set to (0, 1) and for a P-picture or B-picture, ($w_{temporal}$, $w_{spatial}$) are set to (0.5, 0.5). It is noted that in this study the smaller the fitness function value is, the better the error concealment performance will be.

C. Genetic operations

The three basic genetic operations, namely, reproduction, crossover, and mutation, are employed. Reproduction can be performed by selecting the parent chromosomes with smaller fitness function values into the mating pool for generating new offspring bit strings by using the crossover and mutation operations. For the crossover operation, the two parent chromosomes are crossovered via string segments. Here the crossover probabilities for the 8 bits of each bit string segment are assigned to be (1/16, 1/8, 3/16, 1/4, 5/16, 3/8, 7/16, 1/2), respectively. The mutation operation is realized by performing a bitwise shift operation on the binary bit string, and the mutation probability P_M is set to 0.001.

GAs for error concealment will be performed on the concealed blocks for a corrupted/lost block iteratively until the stopping criterion is satisfied. The stopping criterion is either the percentage of the fitness function value improvement between two successive iterations is smaller than a threshold or the number of GA iterations is larger than another threshold. The chromosome (a concealed block candidate) with the smallest fitness function value will be finally determined to be the concealed block of the corrupted/lost block. As a summary, the proposed genetic algorithm approach to error concealment is summarized as Fig. 4.

3. SIMULATION RESULTS

Four test image sequences "Salesman," "Table Tennis," "Flower," and "Football" with different bit error rates (BER) and different average lengths of burst errors (N_{ave}) are used to evaluate the performance of the proposed approach. Each sequence consists of 30 image frames, a gop (group of pictures) consists of 9 pictures (N = 9), and the number of B-pictures between I- or P-pictures is 2 (M = 3). The average length of burst errors N_{ave} is given by $N_{ave} = \sum_{i=1}^{N} i\,P_i$, where P_i is the probability of a burst error containing i successive error bits with $\sum_{i=1}^{N} P_i = 1$. Here N is set to 5 and N_{ave} will lie within the range (1, 5).

The peak signal to noise ratio (PSNR) is employed in this study as the objective performance measure. The PSNR of the i-th picture in an MPEG image sequence, denoted by $PSNR_{P,i}$, is defined as:

$$PSNR_{P,i} = (4 \times PSNR_{Y,i} + PSNR_{cb,i} + PSNR_{cr,i})/6,$$

where $PSNR_{Y,i}$, $PSNR_{cb,i}$ and $PSNR_{cr,i}$ are the corresponding PSNR values of the Y, C_b and C_r components of the i-th picture, respectively. The average PSNR of an MPEG image sequence containing n pictures, denoted by $PSNR_{seq}$, is given by:

$$PSNR_{seq} = \sum_{i=1}^{n} (PSNR_{P,i}) / n.$$

The set of weighting coefficients of the spatial fitness function $\{w_1, w_2, w_3, w_4, w_5\}$ is set to {0.35, 0.35, 0.1, 0.1, 0.1} when the believable blocks are "uniform," and {0.4, 0.4, 0.67, 0.67, 0.67} when the believable blocks are "not uniform."

To compare the performances of existing error concealment and the proposed approach, four existing error concealment methods [10], [12], [13] are implemented in this study. The four existing error concealment methods include: (1) zero-substitution, which simply replaces all pixels in a corrupted/lost block by zeros, denoted by Zero-S; (2) spatial error concealment using multi-directional interpolation, denoted by Spatial-M; (3) spectral error concealment exploiting interblock correlation, denoted by Spatial-I; and (4) hybrid error concealment for digital simulcast AD-HDTV decoder, denoted by Hybrid-A. In terms of $PSNR_{seq}$ in dB, the performance comparison between the four existing error concealment approaches and the proposed approach for the "Football" image sequence is listed in Table 1. As a subjective measure of the quality of the concealed images, the original and concealed images with BER = 0.05% and $N_{ave} = 4$ for the "Football" sequence are shown in Fig. 5. It is noted that the blurring effect of the concealment results (P-pictures) is due to the accumulation (propagation) effect of interframe coding used in MPEG images.

To show the effectiveness of the second (backtracking) procedure of the proposed error detection approach, the simulation results $PSNR_{seq}$ for the "Football" sequence with different BER and N_{ave} of the proposed approach without and with the second (backtracking) procedure are shown in Table 2. To illustrate the effectiveness of the proposed (hybrid) objective cost function for error concealment, the simulation results for the "Football" sequence using the cost function AIDB(C), the spatial error concealment measure $f_{spatial}(\cdot)$, and the proposed error concealment cost function $f(\cdot)$ are listed in Table 3.

4. CONCLUDING REMARKS

Based on the simulation results obtained in this study, several phenomena can be observed. (1) The more smooth the original image is, the better the corresponding error detection and concealment results are. (2) The thresholds and weighting coefficients used will affect the performance of the proposed approach. (3) As BER increases, the total number of corrupted/lost blocks in an MPEG image sequence will usually increase, and the time required to obtain the concealed results will increase accordingly. (4) Based on the simulation results shown in Table 3, the corresponding concealment results for the proposed cost function for error concealment $f(\cdot)$ are better than that for the cost functions AIDB(C) or $f_{spatial}(\cdot)$. (5) Based on the simulation results shown in Table 2, the corresponding concealment results of the proposed error detection approach containing two successive procedures are better than that of the proposed error detection approach containing only the first procedure. (6) Based on the simulation results shown in Table 1 and Fig. 5, the concealment results of the proposed approach are better than that of the four existing error concealment approaches, namely, Zero-S, Spatial-M, Spectral-I, and Hybrid-A.

In this study, the detection and concealment approach to transmission errors in MPEG images is proposed. Based on simulation results obtained in this study, the proposed approach can recover high-quality MPEG images from the corresponding corrupted MPEG images, without increasing the transmission bit rate. This shows the feasibility of the proposed approach.

REFERENCES

[1] H. M. Hang and J. W. Woods, *Handbook of Visual Communications*. San Diego, CA: Academic Press, 1995.

[2] A. M. Tekalp, *Digital Video Processing*. New Jersey: Prentice Hall PTR, 1995.

[3] D. L. Gall, "MPEG: a video compression standard for multimedia applications," *Commun. of the ACM*, vol. 34, no. 4, pp. 46-58, 1991.

[4] ISO-IEC JTC1/SC29/WG11/602, Coding of Moving Pictures and Associated Audio, Recommendation H.262, 1993.

[5] S. Roman, *Coding and Information Theory*. New York: Springer-Verlag, 1992.

[6] C. H. Chang and J. J. Leou, "Detection and correction of transmission errors in DPCM images," *IEEE Trans. on Circuits and Systems for Video Tech.*, vol. 5, no. 2, pp. 166-171, 1995.

[7] C. Y. Chang and J. J. Leou, "Detection and elimination of 2-D transmission error patterns in DPCM images," *IEEE Trans. on Commun.*, vol. 44, no. 10, pp. 1251-1256, 1996.

[8] W. L. Shyu and J. J. Leou, "Detection and correction of transmission errors in facsimile images," *IEEE Trans. on Commun.*, vol. 44, no. 8, pp. 938-948, 1996.

[9] H. Sun and W. Kwok, "Concealment of damaged block transform coded images using projections onto convex sets," *IEEE Trans. on Image Processing*, vol. 4, no. 4, pp. 470-477, 1995.

[10] W. Kwok and H. Sun, "Multi-directional interpolation for spatial error concealment," *IEEE*

Trans. on Consumer Electronics, vol. 39, no. 3, pp. 455-460, 1993.

[11] W. M. Lam and A. R. Reibmain, "An error concealment algorithm for images subject to channel errors," *IEEE Trans. on Image Processing*, vol. 4, no. 5, pp. 533-542, 1995.

[12] S. S. Hemami and T. H. Y. Meng, "Transform coded image reconstruction exploiting interblock correlation," *IEEE Trans. on Image Processing*, vol. 4, no. 7, pp. 1023-1027, 1995.

[13] H. Sun, K. Challapalli, and J. Zdepski, "Error concealment in digital simulcast AD-HDTV decoder," *IEEE Trans. on Consumer Electronics*, vol. 38, no. 3, pp. 108-118, 1992.

[14] J. W. Kim, J. W. Park, and S. U. Lee, "Error-resilient decoding of randomly impaired MPEG-2 bit stream," *SPIE*, vol. 2227, pp. 78-88, 1996.

[15] D. E. Goldberg, *Genetic Algorithms: Search, Optimization and Machine Learning*. Reading, Massachusetts: Addison-Wesley, 1989.

[16] H. C. Shyu, "Detection and concealment of transmission errors in MPEG images," *Master Thesis*, Institute of Computer Science and Information Engineering, National Chung Cheng University, Chiayi, Taiwan, Republic of China, 1996.

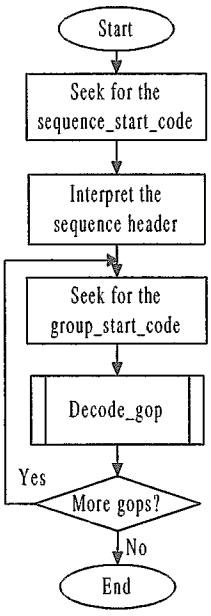

Fig. 1. The Decode_sequence procedure.

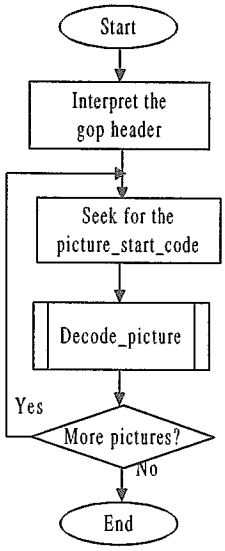

Fig. 2. The Decode_gop procedure.

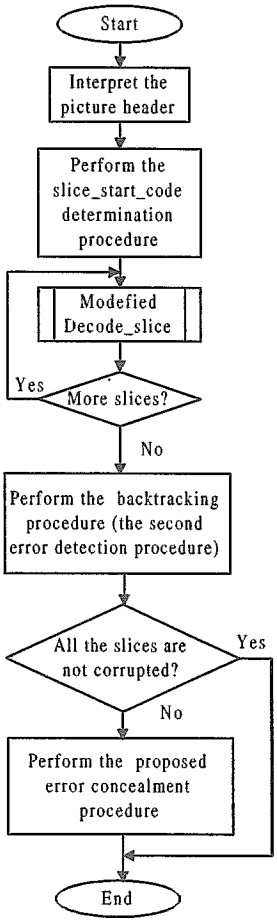

Fig. 3. The Decode_picture procedure.

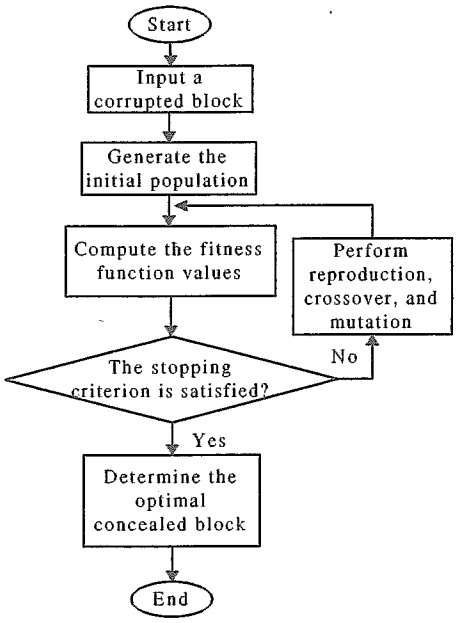

Fig. 4. The proposed genetic algorithm approach to error concealment.

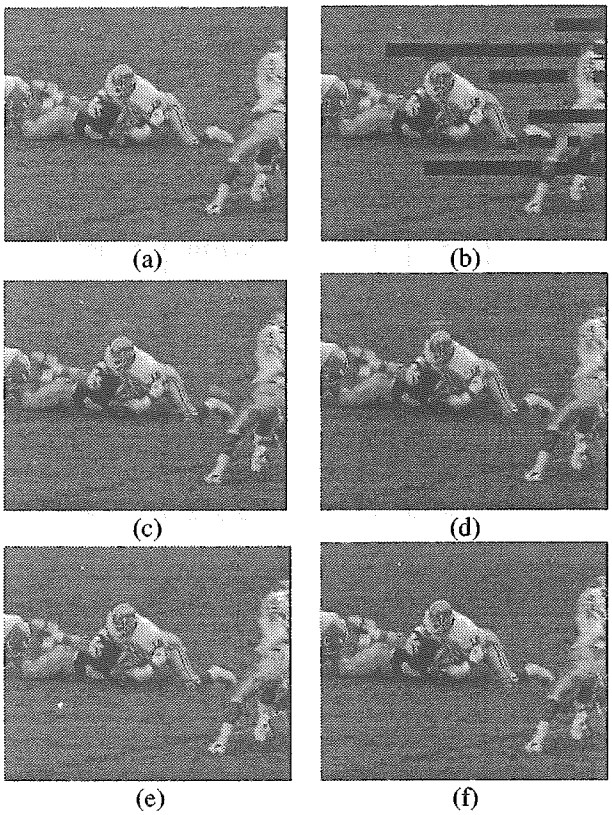

Fig. 5. The original and concealed MPEG images (the Y component) of a P-picture within the "Football" sequence with BER=0.05% and N_{ave} = 4: (a) the original image; (b)-(f) the concealed images by Zero-S, Spatial-M, Spectral-I, Hybrid-A, and the proposed approach, respectively.

Table 1. The simulation results $PSNR_{seq}$ for the "Football" sequence with different BER and N_{ave} of the four existing error concealment approaches and the proposed approach.

BER	N_{ave}	$PSNR_{seq}$					
		No loss	Zero -S	Spatial -M	Spectral -I	Hybrid -A	Pro-posed
0.01 %	1	38.67	14.45	22.744	21.591	25.453	27.296
	2	38.67	14.63	22.103	20.495	25.860	27.845
	3	38.67	16.67	22.799	23.328	26.467	28.411
	4	38.67	18.70	23.864	24.273	26.500	28.533
	5	38.67	19.31	25.278	25.976	27.797	29.696
0.03 %	1	38.67	11.81	19.209	19.021	25.365	27.189
	2	38.67	14.66	22.922	22.852	26.064	27.779
	3	38.67	15.99	23.453	23.082	25.896	28.243
	4	38.67	15.25	23.381	23.109	27.146	29.234
	5	38.67	17.21	24.299	23.889	27.189	29.433
0.05 %	1	38.67	11.82	15.237	18.404	23.885	25.763
	2	38.67	11.97	18.841	20.661	24.816	26.931
	3	38.67	13.14	20.209	22.561	25.279	26.873
	4	38.67	13.32	21.917	21.910	25.093	27.885
	5	38.67	13.56	23.068	23.058	26.436	28.292
0.07 %	1	38.67	11.63	16.238	18.503	24.136	25.304
	2	38.67	11.48	18.888	18.518	23.592	25.509
	3	38.67	12.01	20.031	19.336	24.062	25.947
	4	38.67	14.00	21.176	20.570	25.837	27.775
	5	38.67	13.64	22.323	23.055	26.317	27.543
0.09 %	1	38.67	10.51	14.744	16.458	20.249	22.631
	2	38.67	11.81	15.786	17.824	21.817	24.437
	3	38.67	12.06	18.163	20.520	24.102	26.787
	4	38.67	12.45	19.174	20.643	24.524	27.027
	5	38.67	12.97	19.450	20.411	26.199	27.232
0.1 %	1	38.67	10.33	13.351	15.131	20.410	22.880
	2	38.67	11.01	13.014	16.085	21.076	23.497
	3	38.67	10.86	16.295	18.419	22.727	24.822
	4	38.67	13.19	20.680	20.920	23.259	25.540
	5	38.67	12.02	20.419	20.160	23.901	25.141
0.2 %	1	38.67	9.916	11.397	14.091	18.152	19.008
	2	38.67	10.69	14.697	16.540	20.212	21.264
	3	38.67	10.68	14.860	17.164	20.620	21.519
	4	38.67	10.73	13.687	16.076	21.893	22.712
	5	38.67	11.22	16.786	17.965	23.587	24.298
0.5 %	1	38.67	9.597	10.115	13.238	14.539	16.739
	2	38.67	9.735	11.250	13.923	17.176	18.601
	3	38.67	9.892	12.861	14.271	18.650	19.885
	4	38.67	10.07	14.539	15.450	17.515	19.688
	5	38.67	10.16	12.796	15.898	18.076	20.037

Table 2. The simulation results $PSNR_{seq}$ for the "Football" sequence with different BER and N_{ave} of the proposed approach without and with the second (backtracking) procedure.

BER	N_{ave}	without	with
0.01 %	1	25.532	27.296
	2	25.871	27.845
	3	27.420	28.411
	4	27.797	28.533
	5	28.592	29.696
0.03 %	1	25.450	27.189
	2	25.712	27.779
	3	26.303	28.243
	4	27.624	29.234
	5	27.939	29.433
0.05 %	1	24.087	25.763
	2	24.361	26.931
	3	25.273	26.873
	4	26.027	27.885
	5	26.449	28.292
0.07 %	1	23.383	25.304
	2	23.733	25.509
	3	23.866	25.947
	4	25.819	27.775
	5	25.857	27.543
0.09 %	1	21.126	22.631
	2	22.379	24.437
	3	24.919	26.787
	4	24.873	27.027
	5	25.207	27.232
0.1 %	1	20.791	22.880
	2	21.397	23.497
	3	23.243	24.822
	4	23.856	25.540
	5	23.365	25.141
0.2 %	1	17.692	19.008
	2	20.237	21.264
	3	20.423	21.519
	4	21.133	22.712
	5	22.084	24.298
0.5 %	1	15.551	16.739
	2	17.664	18.601
	3	18.626	19.885
	4	18.644	19.688
	5	18.549	20.037

Table 3. The simulation results $PSNR_{seq}$ for the "Football" sequence with different BER and N_{ave} of the three different cost functions AIDB(C), $f_{spatial}(\cdot)$, and $f(\cdot)$.

BER	N_{ave}	$AIDB(C)$	$f_{spatial}(\cdot)$	$f(\cdot)$
0.01 %	1	21.885	23.525	27.296
	2	21.685	23.777	27.845
	3	25.352	26.157	28.411
	4	25.420	27.606	28.533
	5	26.064	27.450	29.696
0.03 %	1	21.754	23.571	27.189
	2	21.232	23.631	27.779
	3	21.607	24.818	28.243
	4	23.844	26.215	29.234
	5	24.517	26.517	29.433
0.05 %	1	20.477	22.308	25.763
	2	18.790	21.861	26.931
	3	20.793	24.594	26.873
	4	21.897	24.221	27.885
	5	22.368	24.639	28.292
0.07 %	1	19.338	21.304	25.304
	2	19.538	22.240	25.509
	3	18.979	22.149	25.947
	4	21.739	23.671	27.775
	5	21.986	24.308	27.543
0.09 %	1	17.068	20.312	22.631
	2	18.186	20.039	24.437
	3	20.566	23.309	26.787
	4	20.881	22.043	27.027
	5	20.540	23.442	27.232
0.1 %	1	16.441	18.512	22.880
	2	17.589	18.547	23.497
	3	18.989	22.400	24.822
	4	19.467	22.832	25.540
	5	19.137	21.907	25.141
0.2 %	1	15.108	15.968	19.008
	2	17.538	19.495	21.264
	3	17.232	19.964	21.519
	4	17.216	19.951	22.712
	5	17.040	20.124	24.298
0.5 %	1	13.545	13.634	16.739
	2	15.834	16.320	18.601
	3	16.121	16.994	19.885
	4	16.253	17.545	19.688
	5	15.387	16.889	20.037